Macromolecules

Article

pubs.acs.org/Macromolecules

Water-Soluble Poly(γ-propargyl-L-glutamate) Containing Pendant Sulfonate Ions and Terminal Fluorophore: Aggregation-Enhanced Emission and Secondary Structure

Ke-Ying Shih, Tai-Shen Hsiao, Shiang-Lin Deng, and Jin-Long Hong*

Department of Materials and Optoelectronic Science, National Sun Yat-Sen University, Kaohsiung 804, Taiwan

Supporting Information

ABSTRACT: Tetraphenylthiophene (TP) with aggregation-enhanced emission (AEE) property was used as terminal fluorophore of the water-soluble poly(γ-propargyl-L-glutamate) (PPLG)-based polymers of TP-iPPLGs to probe the relationship between the secondary structure (α-helix) of polypeptides and the AEE-related emission behavior. Intermolecular aggregation of the terminal TP unit in TP-iPPLG is sterically blocked by the large α-helical PPLG chains, leading to the weak AEE-related fluorescence in water. In contrast, the intermolecular approach between the terminal TP units of TP-iPPLG is accessible if TP was connected by peptide chin in random coil structure. Therefore, the helix-to-coil transition induced in the alkaline aqueous solution successfully enhances the emission intensity of the TP-iPPLG solution. The pH-induced conformation change in relationship to the AEE-related emission behavior is therefore evaluated in this study.

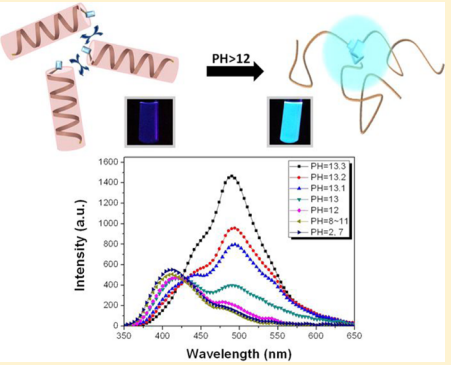

INTRODUCTION

Synthetic polypeptides are mimics of natural peptides and able to form stable secondary structures (e.g., α-helix, β-sheets, and random coil) in solution and solid state.[1−3] As the cornerstone of the three-dimensional architecture of proteins, the α-helical structure functioned to regulate numerous biological activities. The unique folding/unfolding property and the rigid rodlike morphology have made the α-helix the subject of intense study and building block in the design of therapeutics and molecular assemblies.[4−13] However, the usefulness of these structures is limited because of their poor aqueous solubility and processability. Therefore, interest has been largely focused on the design and synthesis of water-soluble α-helical polypeptide. Therefore, charged amino groups[14,15] and cyclodextrin[16] have been incorporated with polypeptides as the side chains to render in the good water solubility. The ultrastable, water-soluble α-helical polypeptides[14] can be produced by elongating charge-containing amino acid side chains to position the charges distant from the polypeptide backbone.

As fluorescence (FL) spectroscopy constitutes one of the most powerful tools to study the aggregation of polymers, traditional fluorescent probes such as carbazolyl,[17] dansyl,[18] and pyrene[19] have been chemically incorporated with poly(γ-benzyl-L-glutamate) (PBLG) to monitor the chain conformations of PBLG in solution. For example, the absence of excimer emission in the pyrene-labeled poly(ethylene glycol)-*b*-PBLG[19] indicated that the pyrene groups were separated from each other in the self-assembled structure. A study on triblock PBLG−polyfluorene−PBLG copolymers[20] suggested that formations of rod−rod−rod and coil−rod−coil conformations depend on the solvent casting history and the morphological variations resulted in different emission and FL decay behaviors. Study on the fluorophore-labeled PBLG provided routes for the evaluation of aggregation behavior of the peptide chains.

Traditional planar fluorophores (e.g., pyrene and anthracene) are generally weakly emissive in the solid state. In contrast, noncoplanar silole molecule (1-methyl-1,2,3,4,5-pentaphenylsilole)[21,22] was found to have strong emission in the aggregated solution and solid states despite that it is nonemissive in the dilute solution state. Aggregation-induced emission (AIE) was therefore designated for this peculiar phenomenon in view that the originally nonluminescent solution of silole can be tuned to emit strongly when aggregates formed by nonsolvent inclusion. Since the first discovery of the silole system, several organic and polymeric materials[23−28] with AIE or aggregation-enhanced emission (AEE) properties have been prepared and characterized. With chemical structure similar to silole, tetraphenylthiophene (TP) and TP-derived organic and polymeric materials[29−31] were developed in our lab, and their AIE and AEE characters were identified. Also, this TP fluorophore was served as the terminal and central fluorophores of PBLG-based polymers of TP1PBLG and TP2PBLG,[32] respectively, to probe the relationship between the secondary structure (α-helix) of polypeptides and the AEE-related fluorescence. Mainly, intermolecular aggregation of the central TP units in the disubstituted TP2PBLGs is sterically blocked by the large α-helical PBLG chains, leading to the reduced AEE-oriented

Received: April 29, 2014
Revised: June 3, 2014
Published: June 12, 2014

   dx.doi.org/10.1021/ma500886v | Macromolecules 2014, 47, 4037−4047

Scheme 1. Chemical Structure of TP-iPPLGs and the Feasibility of Intermolecular Aggregation among TP Terminals Connected by Different Secondary Structures

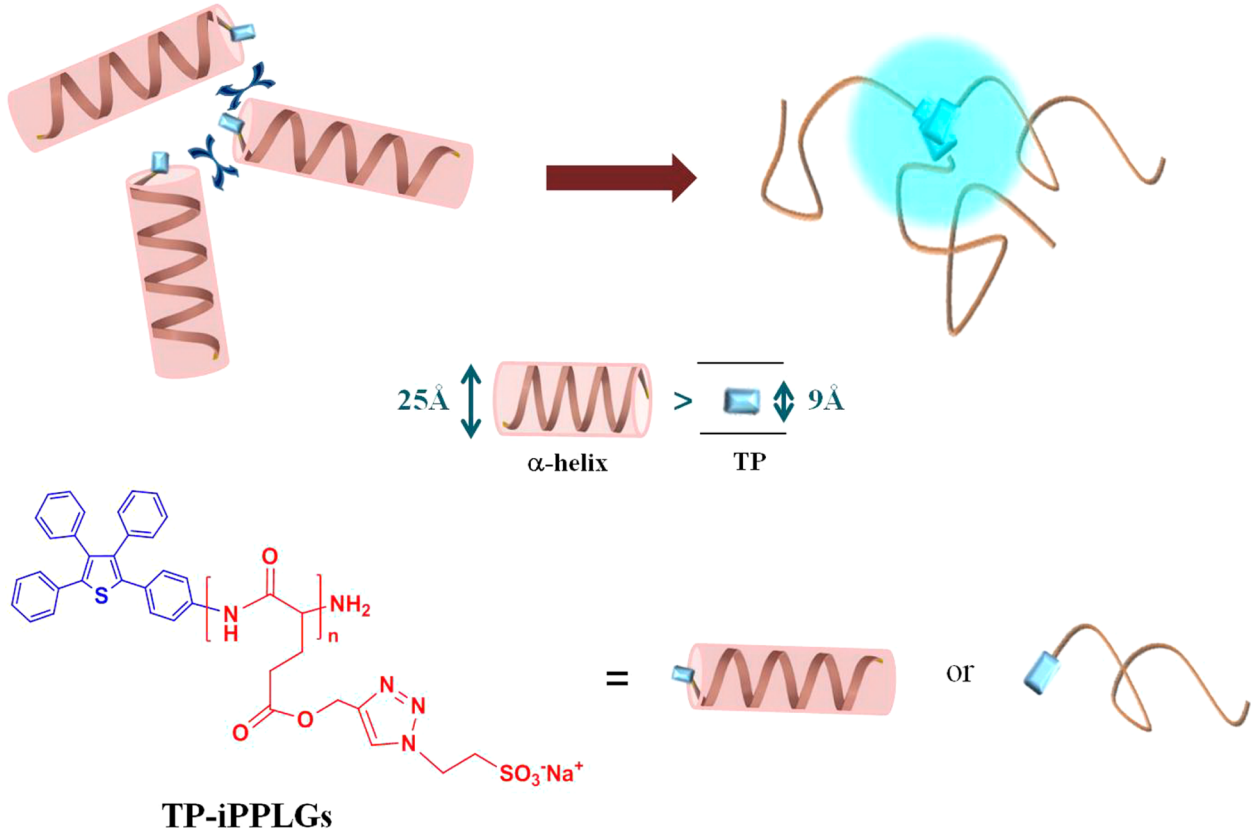

emission. By adding trifluoroacetic acid (TFA), the rigid helical chain of TP2PBLG can be transformed into flexible random coil structure; therefore, adding TFA largely intensified the emission intensity of TP2PBLG since intermolecular aggregation of the TP centers in random-coil chain can be readily achieved. Comparatively, the terminal TP units in the monosubstituted TP1PBLGs have no problem in approaching each other, resulting in strong emission intensity. The secondary structure of polypeptides is therefore correlated with the AEE activity.

In contrast to the water-insoluble TP1PBLG and TP2PBLG,[32] a new water-soluble polypeptide of TP-iPPLG (Scheme 1) containing an AEE-active TP terminal and ionic sulfonate side groups were prepared and characterized in this study. Instead of the commonly used organic charged amino[14,15] or β-cyclodextrin (CD)[16] side groups, ionic sodium sulfonate groups were introduced through the facile click reaction and were used as the side chains of TP-iPPLGs to deliver the desired water solubility of the peptide polymers. These ionic TP-iPPLGs provide access to study the influence of sulfonate side groups on the secondary structure of the peptide chain, and the relation between AEE-related emission behavior and secondary structure of peptide chain can be explored. Theoretically, the AEE-related emission of TP-iPPLG is strongly correlated to the aggregation tendency of the TP terminals, which in turn are affected by the steric shielding imposed by the neighboring peptide chains. It is envisaged that the two-dimensional α-helical rod, which has diameter larger than the molecular length of the TP terminal, affords effective steric shielding on the TP terminals and thus is effective in preventing intermolecular aggregation of the TP units. In contrast, no serious steric shielding effect is expected when TP terminals are connected by peptide chains in flexible random coil structure. Readiness of the fluorescent TP units to undergo intermolecular aggregation will affect the AEE-related emission behavior. By varying the secondary structure in alkaline solution, the corresponding helix-to-coil transition occurs to result in TP-iPPLG with random coil chains; with them mutual approaches of the TP terminals are accessible, resulting in enhanced emission with the prevailing AEE effect. The fluorescence response can then be measured, and the relationship between AEE-related emission behavior and secondary structure of the water-soluble polypeptide can be therefore identified.

EXPERIMENTAL SECTION

Materials. All reagents and chemicals were purchased from Aldrich Chemical Co. and used as received. DMF was refluxed and distilled over CaH_2 under reduced pressure to a flask containing alumina and was used directly after distillation. CuBr (98%, Aldrich) was stirred overnight in acetic acid, filtered, washed with ethanol and diethyl ether, and dried in vacuo before use. Compounds of $TPNH_2$,[32] SAES,[31] and γ-propargyl-L-glutamate *N*-carboxyanhydride (PLG-NCA)[33,34] were prepared according to the reported procedures. Detailed procedures for the ring-opening polymerization and click reaction (Scheme 2) are given below.

Ring-Opening Polymerization of *N*-Carboxyanhydride To Prepare TP-PPLGs. Preparation of TP-PPLG(L) was used as an example to illustrate its preparation procedures as follows: a solution of PLG-NCA (3 g, 14.2 mmol) in anhydrous DMF (20 mL) was stirred and bubbled with argon gas for 20 min before a solution of $TPNH_2$ (0.03 mL, 0.48 mmol) in anhydrous DMF (5 mL) was added. After stirring for 2 days at room temperature, the polymer was precipitated from diethyl ether and dried in a vacuum oven. The

dx.doi.org/10.1021/ma500886v | *Macromolecules* 2014, 47, 4037−4047

Scheme 2. Ring-Opening Polymerization of PLG-NCA Monomer by a $TPNH_2$ Initiator and the Following Click Reaction to Obtain TP-iPPLG

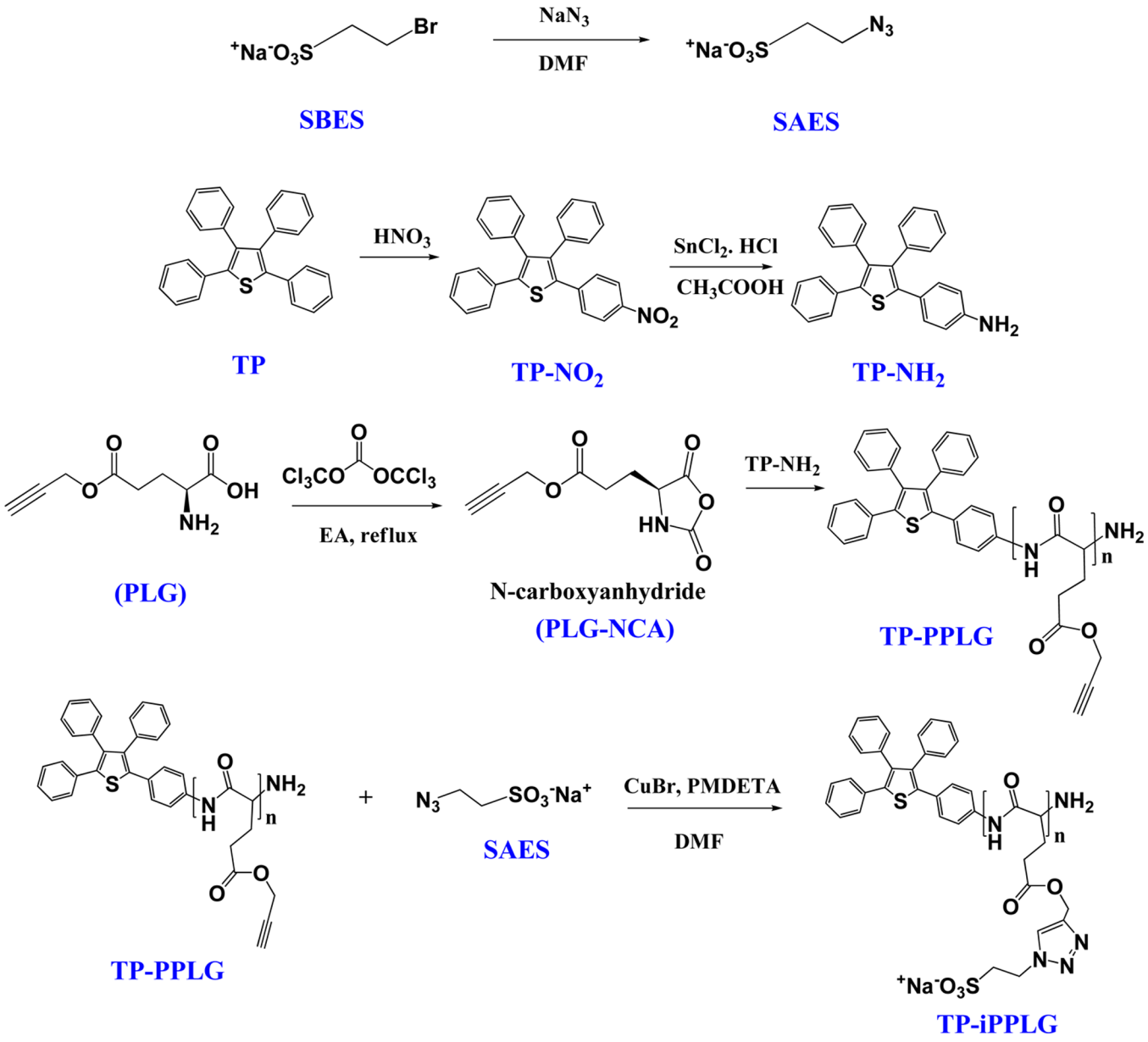

syntheses of TP-PPLG(H) was operated by the same procedure but with different formulation. TP-PPLG(L): ^{1}H NMR (500 MHz, CD_2Cl_2): δ 8.34 (broad, 1H, H_f), 7.5−7.03 (broad, 19H, H_g), 4.70 (s, 2H, H_b), 3.99 (broad, 1H, H_e), 2.62 (broad, 2H, H_c), 2.50 (s, 1H, H_a), 2.32−2.19 (broad, 2H, H_d) (Figure 2a). ^{13}C NMR (125 MHz, CD_2Cl_2): δ 177.0, 173.3, 132−128, 78.7, 75.9, 57.3, 52.8, 31.4, 25.8. (Figure 1a). TP-PPLG(H): ^{1}H NMR (500 MHz, CD_2Cl_2): δ 8.21 (broad, 1H, H_f), 7.25−6.9 (broad, 19H, H_g), 4.61 (s, 2H, H_b), 3.94 (broad, 1H, H_e), 2.61 (broad, 2H, H_c), 2.48 (s, 1H, H_a), 2.23−2.11 (broad, 2H, H_d) (Figure S1a, Supporting Information). ^{13}C NMR (125 MHz, CD_2Cl_2): δ 177.0, 173.9, 132−128, 78.2, 75.9, 57.3, 52.8, 31.4, 25.8 (Figure S2a).

Preparations of TP-iPPLGs by Click Reaction. Preparation of TP-iPPLG(L) was used as an example to illustrate its preparation procedures as follows: SAES (0.57 g, 3.29 mmol), TP-PPLG(L) (0.5 g, 2.99 mmol), and CuBr (0.04 g, 0.3 mmol) were dissolved in DMF (20 mL) in a two-neck flask equipped with a magnetic stirrer and a condenser. After three freeze−thaw−pump cycles, *N,N,N′,N″,N″*-pentamethyldiethylenetriamine (PMDETA) (0.063 mL, 0.3 mmol) was added, and the whole reaction mixture was subjected to another cycle of freeze−thaw−pump. The reaction was then performed at 50 °C under argon for 24 h. After cooling to room temperature, the resultant mixtures were passed through a neutral alumina column to remove the copper catalysts. The eluent was concentrated by rotary evaporation before precipitation from diethyl ether. The precipitate was filtered off and dried under vacuum at room temperature to obtain the final product. The syntheses of TP-iPPLG(H) was operated by the same procedure but with different formulation. TP-iPPLG(L): ^{1}H NMR (500 MHz, d_6-DMSO): δ 8.18 (broad, 1H, $H_{f'}$), 8.06 (s, 1H, $H_{a'}$), 7.48−6.98 (broad, 19H, $H_{g'}$), 5.08 (s, 2H, $H_{b'}$), 4.65 (broad, 2H, H_h), 4.57 (broad, 2H, H_i), 3.02 (broad, 1H, $H_{e'}$), 2.31 (broad, 2H, $H_{c'}$), 1.89−1.74 (broad, 2H, $H_{d'}$) (Figure 2b). ^{13}C NMR (125 MHz, d_6-DMSO): δ 175.0, 173.3, 142.3, 131.1−125.7, 125.3, 67.4, 57.3, 51.6, 46.6, 29.7, 26.9. (Figure 1b). TP-iPPLG(H): ^{1}H NMR (500 MHz, d_6-DMSO): δ 8.16 (broad, 1H, $H_{f'}$), 8.06 (s, 1H, $H_{a'}$), 7.25−6.85 (broad, 19H, $H_{g'}$), 5.08 (s, 2H, $H_{b'}$), 4.56 (broad, 2H, H_h), 4.49 (broad, 2H, H_i), 3.02 (broad, 1H, $H_{e'}$), 2.39−2.23 (broad, 2H, $H_{c'}$), 2.03−1.82 (broad, 2H, $H_{d'}$) (Figure S1b). ^{13}C NMR (125 MHz, d_6-DMSO): δ 175.0, 173.3, 142.3, 131.1−125.7, 125.4, 67.4, 55.1, 51.7, 46.6, 30.3, 26.3 (Figure S2b).

dx.doi.org/10.1021/ma500886v | *Macromolecules* 2014, 47, 4037−4047

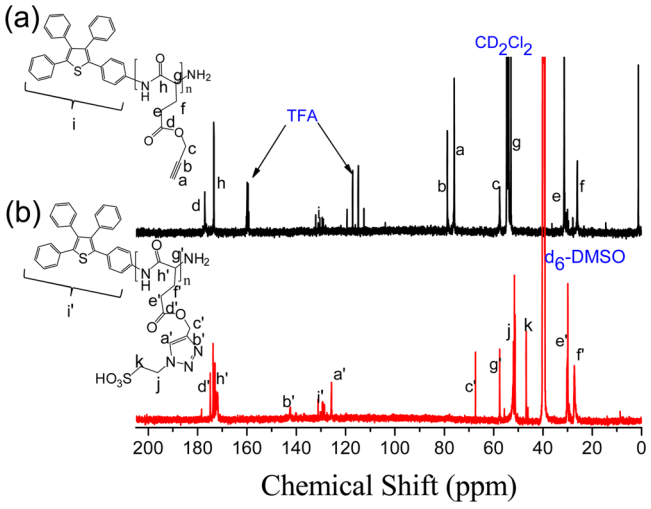

Figure 1. ^{13}C NMR spectra of (a) TP-PPLG(L) (in CD_2Cl_2 + 15 vol % TFA) and (b) TP-iPPLG(L) (in d_6-DMSO).

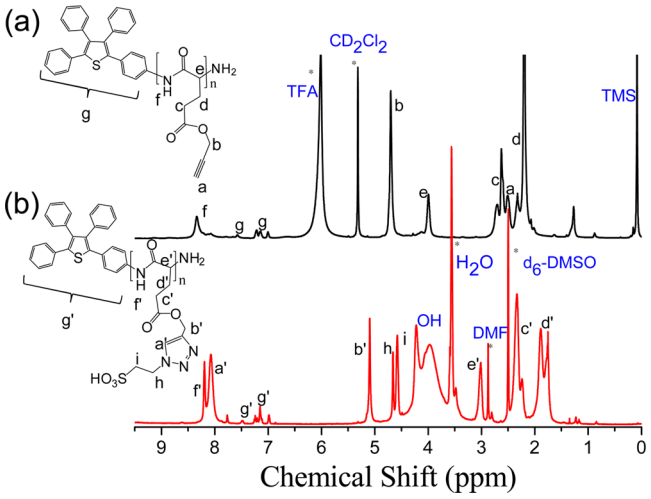

Figure 2. ^1H NMR spectra of (a) TP-PPLG(L) (in CD_2Cl_2 + 15 vol % TFA) and (b) the protonated TP-iPPLG(L) (in d_6-DMSO).

Measurements. ^1H NMR spectra were recorded at room temperature using a Bruker AM 500 (500 MHz) spectrometer with tetramethylsilane (TMS) as the external standard. ^{13}C CP-MAS NMR spectra were acquired on a Bruker 14.1 T wide-bore Avance III spectrometer equipped with a 4 mm double-resonance magic-angle-spinning (MAS) probe head. The Larmor frequency used for ^{13}C NMR is 150.92 MHz. The samples were spun at 12 kHz. FTIR spectra were recorded from a Bruker Tensor 27 FTIR spectrophotometer; 32 scans were collected at a spectral resolution of 1 cm^{-1}. The solid polymer powders were mixed with KBr before being pressed to make pellets for measurement. Mass spectra were obtained from a Bruker Daltonics Autoflex III MALDI-TOF mass spectrometer and operated by the following voltage parameters: ion source 1, 19.06 kV; ion source 2, 16.61 kV; lens, 8.78 kV; reflector 1, 21.08 kV; reflector 2, 9.73 kV. A wide-angle X-ray diffraction (WAXD) pattern was obtained from a Siemens D5000 X-ray diffractometer with a source of Cu Kα ($1^1/_4$ 0.154 nm) radiation at 40 kV and 30 mA. Diffraction patterns were collected with a scan rate of 3 s per 0.1° in the 2θ ranges of 2°−40°. The UV−vis absorption spectra were recorded with an Ocean Optics DT 1000 CE 376 spectrophotometer. The PL emission spectra were obtained from a LabGuide X350 fluorescence spectrophotometer using a 450 W Xe lamp as the continuous light source. A small quartz cell with dimensions 0.2 × 1.0 × 4.5 cm^3 was used to accommodate the solution sample. A "right angle" geometry that fluorescence was collected at right angle to the excitation beam was used in the spectral measurement. Solution quantum yield in water was determined by comparison with a quinine sulfate standard solution (10^{-4} M in 1 N H_2SO_4). The integrating sphere was used to measure the quantum yields of the solid samples. Circular dichroism spectra were recorded using a JASCO J-810 spectrometer, with sample in deionized water at a concentration of 10^{-4} M. Chain dimension of the α-helical structure was calculated from the minimum-energy conformation simulated from the Materials Studio software.

RESULTS AND DISCUSSION

Synthesis of Water-Soluble, Ionic Polymer of TP-iPPLG. The water-soluble TP-iPPLG polymers were synthesized according to the procedures illustrated in Scheme 2. The facile click reaction between azide-functionalized SAES and the alkyne side groups of TP-PPLG is the key step to generate the ionic sulfonate side groups of the final TP-iPPLG products. Primarily, three key reactants including SAES, TP-PPLG, and the AIE-active initiator of TP-NH_2 are prerequisite for the preparation of the desired TP-iPPLG. Two polymeric TP-PPLGs with low and high MWs were prepared from the ring-opening polymerization of *N*-carboxyanhydride monomer of PLG-NCA by the AIE-active initiator of TP-NH_2. The propargyl side group of TP-PPLG was then "clicked" by the azide group of SAES, resulting in two products of TP-iPPLG(L) and TP-iPPLG(H) with relatively low and high MWs, respectively. Here, the cyclic monomer of PLG-NCA needed to be prepared from the facile cyclization of propargyl glutamate (PLG) in the presence of triphosgene while another key intermediate of TP-NH_2 was obtained from a two-step reaction procedure, starting from the initial nitration of TP followed by reduction of the nitro group to obtain the desired amino function in $TPNH_2$. The azide-functionalized SAES was synthesized by a simple substitution reaction between sodium azide (NaN_3) and SBES. All the intermediate reactant and final products were carefully identified, and the detailed spectral data are included in the Supporting Information.

FTIR spectroscopic analysis can be primarily applied to confirm the success of the click reaction, by which the neutral TP-PPLG can be converted to ionic TP-iPPLG. FTIR spectra revealed the complete disappearance of the characteristic signals for the azide and acetylene groups (Figure 3). The signals at 2130 cm^{-1}, representing the alkyne group of TP-PPLG(L), and 2105 cm^{-1}, representing the azide group of SAES, were absent in the spectrum of TP-iPPLG(L). A signal

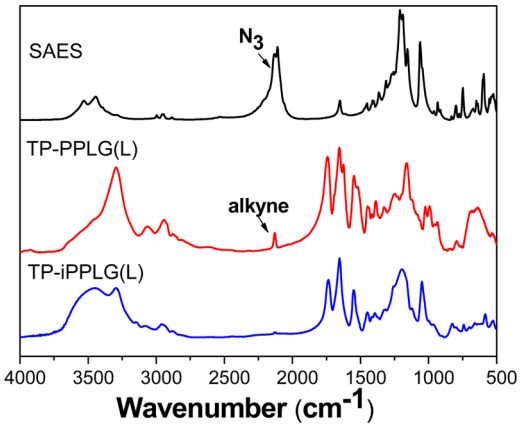

Figure 3. Solid FTIR spectra of SAES, TP-PPLG(L), and TP-iPPLG(L).

dx.doi.org/10.1021/ma500886v | *Macromolecules* 2014, 47, 4037−4047

Table 1. Molecular Weights of TP-PPLG and TP-iPPLG Species Determined from MALDI-TOF and ^{1}H NMR Spectroscopies

	from MALDI-TOF[a]				from ^{1}H NMR	
	M_n[a]	M_w[a]	PDI[a]	N[b]	M_n	N[b]
TPPPLG(L)	2900 (±3%)	3050 (±1%)	1.05	17	3480 (±4%)	20
TPPPLG(H)	4490 (±1%)	4840 (±2%)	1.08	27	5170 (±1%)	31
TP-iPPLG(L)					7020 (±3%)	20
TP-iPPLG(H)					10370 (±1%)	30

[a] M_n = number-average molecular weight, M_w = weight-average molecular weight, PDI = polydispersity. [b] N = number of repeat units.

for the amide I groups of the TP-PPLG(L) at 1660 cm^{-1} also appeared in the spectrum of TP-iPPLG(L). The well-defined structures of the neutral TP-PPLGs were confirmed in the corresponding MALDI-TOF MS spectra (Figure S4), which revealed only one apparent distribution for both TP-PPLG(L) and TP-PPLG(H). Unfortunately, no MS peaks can be resolved from the ionic TP-iPPLG polymers because the difficulty to find appropriate matrix to overcome the strong electrostatic interaction forces among the sulfonate pendant groups of the ionic polymers. The MWs of the neutral TP-PPLG species from the MALDI-TOF analysis are listed in Table 1, which indicates that number (N) of the repeat unit in the low- and high-MW TP-PPLG(L) and TP-PPLG(H) are 17 and 27, respectively. To unambiguously determine the MWs of the ionic TP-iPPLG(L) and TP-iPPLG(H) polymers, ^{13}C and ^{1}H NMR spectroscopies were further applied.

Figure 1 presents the ^{13}C NMR spectra of TP-PPLG(L) and TP-iPPLG(L). The ^{13}C NMR spectrum of TP-PPLG(L) in CD_2Cl_2/TFA (Figure 1a) revealed signals for the ester C═O [C_d] and amide C═O carbon [C_h] atoms at 177 and 173.3 ppm, respectively, whereas those of the alkyne carbon [C_a and C_b] atoms appeared at the respective positions of 75.9 and 78.7 ppm. The signals for the amino acid α-carbon atoms (C_g) appeared at 52.8 ppm. For TP-iPPLG(L) (Figure 1b), the ester C═O carbon [$C_{d'}$], the amide C═O carbon [$C_{h'}$] and the amino acid α-carbon ($C_{g'}$) atoms resonated at positions in close vicinities of those in the spectrum of TP-iPPLG(L). However, the resonances of the two carbon atoms [$C_{a'}$ and $C_{b'}$] of the triazole ring appeared at 142.3 and 125.3 ppm. No signal of the alkyne carbons (C_a and C_b in Figure 1a) can be detected in Figure 1b, indicating the completeness of the click reaction. In addition, before click reaction the signal for the carbon (C_c, Figure 1a) neighboring to alkyne appeared at 57.3 ppm; after click reaction this signal shifted considerably to 67.4 ppm ($H_{c'}$ in Figure 1b). Results from the ^{13}C NMR spectra indicated that click reaction carried out successfully to result in quantitative transformation from alkyne to triazole ring with sulfonate function.

Initially, MWs of TP-iPPLGs cannot be determined from the ^{1}H NMR spectra because no phenyl proton signal of TP terminal is present in the spectra of TP-iPPLGs in D_2O. The TP terminals buried in the ionic aggregates of TP-iPPLG polymers are supposed to be inert to the stimuli of external magnetic field; thereby, acidic HCl was used to dissociate the ionic interaction, and as expected, the resulting protonated TP-iPPLG showed the resolvable aromatic resonances of the TP units. Figure 2 presents the ^{1}H NMR spectra of TP-PPLG(L) and the protonated TP-iPPLG(L) dissolved in CD_2Cl_2/trifluoroacetic acid (TFA, 15 vol %) and d_6-DMSO, respectively. For TP-PPLG(L), the aromatic protons of the TP initiator resonated as multiplets (H_g in Figure 2a) in the range from 7.03 to 7.5 ppm. The signal for the amide protons [H_f] of TP-PPLG(L) appeared as a singlet at 8.34 ppm; the singlet at 2.50 ppm corresponded to the alkyne protons [H_a]. The resonance peaks of side-chain alkyl CH_2 protons (H_c and H_d) appeared upfield as multiplets between 2.0 and 2.7 ppm. The resonance of the main-chain alkyl CH protons [H_e] appeared as a singlet at 3.99 ppm, which became the resonance peak of TP-iPPLG(L) at 3.02 ppm ($H_{e'}$ in Figure 2b) in d_6-DMSO. For TP-iPPLG(L), the resonance at 8.06 ppm was due to the protons [$H_{a'}$] in the triazole structure resulting from the click reaction, which confirms the successful synthesis of TP-iPPLG(L). For TP-PPLG(L), the signal of the CH_2 [H_b] neighboring to acetylene group was located at 4.7 ppm (Figure 2a), and it shifted downfield significantly to 5.08 ppm ($H_{b'}$ in Figure 2b) for TP-iPPLG(L). The peak area ratio between proton $H_{b'}$ and the aromatic protons $H_{g'}$ can be used to calculate the number-average MW (M_n) of TP-iPPLG(L). The same calculation can be made on TP-iPPLG(H) (Figure S1b), too, and the results listed in Table 1 indicate good correlation between the number (N) of repeat unit of TP-PPLGs and TP-iPPLGs.

Conformational Transformation from the Solid TP-PPLG to the Solid TP-iPPLG. The conformations of the TP-PPLG and TP-iPPLG solids can be evaluated by analyzing the amide absorptions in their FTIR spectra (Figure 4). Analysis of these spectra using the second-derivative technique revealed that the amide I band at 1655 cm^{-1} was characteristic of α-helical secondary structure while for polypeptides possessing a β-sheet conformation, the amide I band was located at 1627 cm^{-1}. Random coil or turn populations were characterized by a signal at 1693 cm^{-1}, and the free C═O unit of the side chain group of PPLG provided a signal at 1740 cm^{-1}. The spectra in

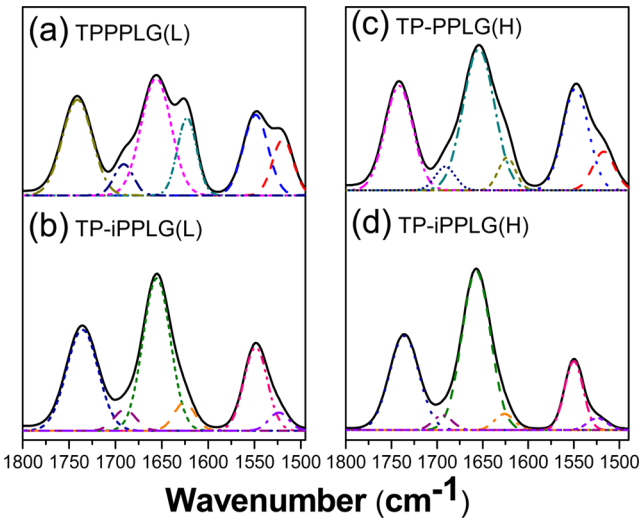

Figure 4. FTIR spectra of (a) TP-PPLG(L), (b) TP-iPPLG(L), (c) TP-PPLG(H), and (d) TP-iPPLG(H).

dx.doi.org/10.1021/ma500886v | Macromolecules 2014, 47, 4037−4047

Table 2. Secondary Structures of TP-PPLG and TP-iPPLG Species Determined from Infrared Spectroscopy

	random coil		α-helix		β-sheet	
sample	ν (cm^{-1})	A_f (%)	ν (cm^{-1})	A_f (%)	ν (cm^{-1})	A_f (%)
TP-PPLG(L)	1691	10.6 (±0.2)	1656	62.7 (±0.2)	1623	26.7 (±0.1)
TP-PPLG(H)	1691	8.7 (±0.1)	1655	80.9 (±0.1)	1623	10.4 (±0.2)
TP-iPPLG(L)	1691	8.8 (±0.1)	1655	80 (±0.1)	1625	11.2 (±0.1)
TP-iPPLG(H)	1691	5.6 (±0.2)	1655	88.2 (±0.1)	1625	6.2 (±0.1)

the range from 1500 to 1800 cm^{-1} were then deconvoluted into a series of Gaussian curves to quantify the fraction of each of the peaks. Table 2 summarizes our results obtained from curve fitting of the amide I group for the random coil, α-helical, and β-sheet structures. The result suggested that increasing MW of the peptide chains tends to promote the rigid α-helical secondary structure. Therefore, high-MW TP-PPLG(H) and TP-iPPLG(H) contain more fractions of α-helical structures than the low-MW analogues of TP-PPLG(L) and TP-iPPLG(L), respectively. This result is similar to the finding reported by Papadopoulos et al. for PBLG.[35] Besides the MW effect, the ionic pendant groups of TP-iPPLGs are also beneficial for the formation of α-helical chain. Therefore, the ionic TP-iPPLGs always have higher fraction of α-helical secondary structure than their neutral precursors of TP-PPLGs. It may be envisaged that the α-helical conformation possesses long intrachain distance between the neighboring ionic side groups; thus, electrostatic repulsion forces can be reduced in the α-helical conformation of TP-iPPLG(L) and TP-iPPLG-(H).

Figure 5 displays the ^{13}C CP/MAS spectra of TP-PPLGs and TP-iPPLGs. The different ^{13}C chemical shifts of the C_α and

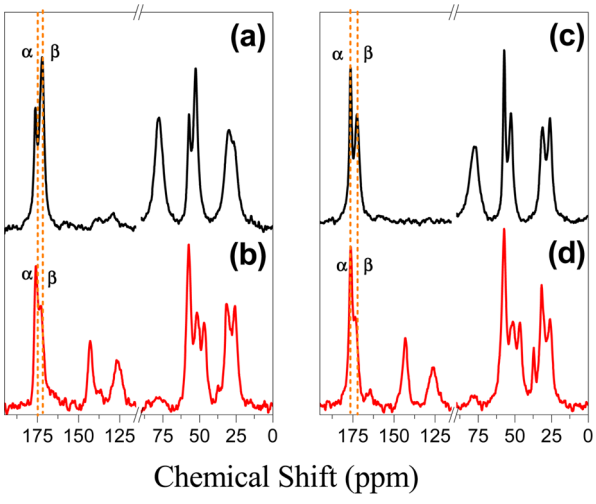

Figure 5. Solid state ^{13}C NMR spectra of (a) TP-PPLG(L), (b) TP-iPPLG(L), (c) TP-PPLG(H), and (d) TP-iPPLG(H).

amide C═O carbon atom nuclei relate to the local conformations of the individual amino acid residues, characterized by their dihedral angles and types of intermolecular and intramolecular H-bonds.[36,37] In the case of TP-PPLGs, the α-helical secondary structure was characterized by the signals of the C_α and amide C═O resonances appeared at 57.5 and 176 ppm, respectively. In the β-sheet conformation, these signals were shifted upfield, by approximately 4−5 ppm, to 52.7 and 172 ppm, respectively.[38] The overlapped C═O absorptions in the range from 167 to 181 ppm can be used to evaluate the relative fraction of α-helical and β-sheet structures; clearly, the ionic TP-PPLGs polymers contain higher fraction of α-helical secondary structure than the neutral TP-iPPLGs. The result coincides with the finding from the FTIR spectra.

Figure 6 displays the WAXD patterns of TP-PPLGs and TP-iPPLGs recorded at room temperature; these diffraction

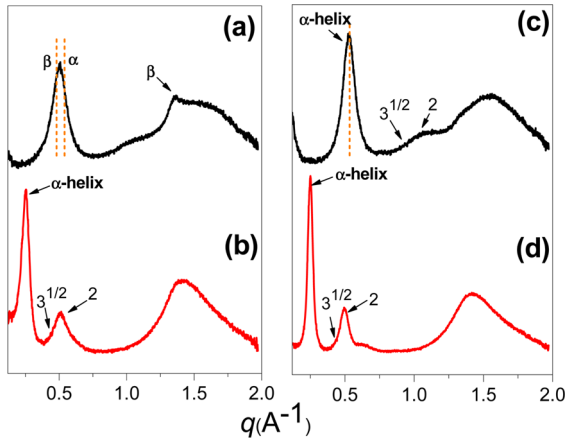

Figure 6. WAXD patterns (recorded at room temperature) of (a) TP-PPLG(L), (b) TP-iPPLG(L), (c) TP-PPLG(H), and (d) TP-iPPLG(H).

patterns exhibit certain differences relative to the content of the secondary structure. For TP-PPLG(L) containing certain fractions of β-sheet chain (cf. Table 2), the sharp peak at q of 1.34 (d = 0.468 nm, the intermolecular distance between adjacent peptide chains within one lamella) was clearly visible (Figure 6a). This result is different from that obtained for TP-PPLG(H) (Figure 6c). The corresponding diffraction at q = 1.34 became inseparate from the amorphous background due to the low content of β-sheet structure. For TP-PPLG(L) and TP-PPLG(H), the three reflections at higher angles, with positions $1:3^{1/2}:4^{1/2}$ relative to the primary peak (q^*), are due to the (10), (11), and (20) reflections of a 2D hexagonal cylindrical packing composed of 18/5 α-helices with a cylinder distance of 1.18 nm.[35] The structure of PPLG has been described as a nematic-like paracrystal with a periodic packing of α-helices in the direction lateral to the chain axis. The broad amorphous region at q = 1.54 is mainly due to the long amorphous side chain group in TP-PPLG. After the click reactions, the ionic TP-iPPLGs contain mainly the α-helical secondary structure; therefore, the WAXD spectra of TP-iPPLG(L) and TP-iPPLG(H) (Figure 6b,d) indicate the presence of three reflections, at positions $1:3^{1/2}:4^{1/2}$ relative to the primary peak diffracted at q = 0.25, which correspond to a 2D hexagonal cylindrical packing with a cylinder distance of 2.51 nm.

Figures 7a and 7b provide a schematic depiction of the α-helical conformation and cylindrical organization of the TP-

dx.doi.org/10.1021/ma500886v | Macromolecules 2014, 47, 4037−4047

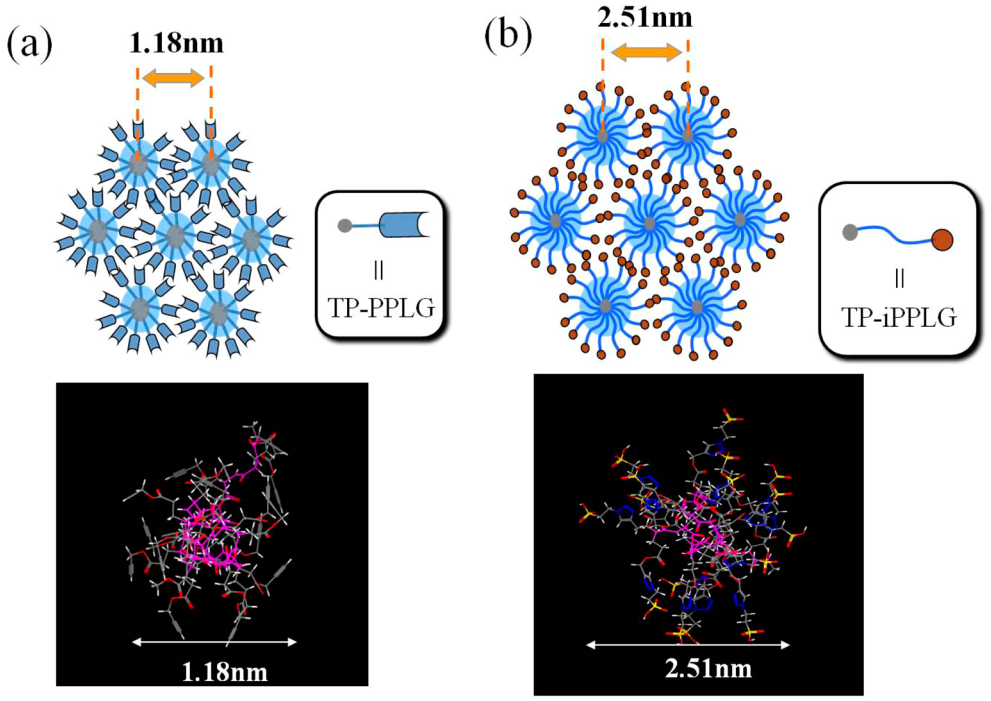

Figure 7. α-Helical rods (upper) and the simulated chain arrangements (lower) of TP-PPLG and TP-iPPLG.

PPLG and TP-iPPLG, respectively. The arrangement of the α-helical conformation for TP-PPLG can be represented by the 2D hexagonal packing (Figure 7a) with a cylinder distance of 1.18 nm, as calculated from the WAXD data, with a characteristic spacing close to the reported value of PPLG.[35] Similar hexagonal packing of cylinders was expected for TP-iPPLG (Figure 7b); however, the cylinder distance for TP-iPPLG is 2.51 nm, as evaluated from a q value of 0.25 according to the WAXD diffraction peak. The observed spacing was close to the thickness (2.5 nm) expected for the repeated packing of a TP-iPPLG bilayer structure, as estimated from the sum of twice the ionic group length (2 × 0.66 nm = 1.32 nm)[16] and the cylinder distance of (1.18 nm) of TP-PPLG (1.32 + 1.18 = 2.5 nm).

Emission Behavior of the TP-iPPLG Polymers. As the main focus of this study, the AEE-related emission behavior was characterized by the solution emission responses toward concentration and aggregation. Effect of concentration was primarily emphasized by the unnormalized solution emission spectra of TP-iPPLGs in water (Figure 8), which exhibited the continuous accession of the emission intensity with increasing concentration. In contrast to the emission quenching caused by solution thickening, solutions of TP-iPPLGs become more emissive with increasing concentration. When concentrations of TP-iPPLG(L) and TP-iPPLG(H) in water were increased from 10^{-5} to 10^{-3} M, more than 10-fold emission enhancements were observed. More drastic emission enhancements were observed in the spectra of the solid samples, which are correlated with the fact that molecular motions are seriously retarded in the solid state. In the solution and solid sates, emissions of the low-MW TP-iPPLG(L) are all higher in intensity than those of the high-MW TP-iPPLG(H) under the same experimental conditions. As suggested above, the rigid α-helical chain is effective in preventing the intermolecular aggregation of the TP terminals; with higher fraction of α-helical chain, the TP-iPPLG(H) polymer therefore emitted with lower intensity than the TP-iPPLG(L) polymer with lower fraction of α-helical chain.

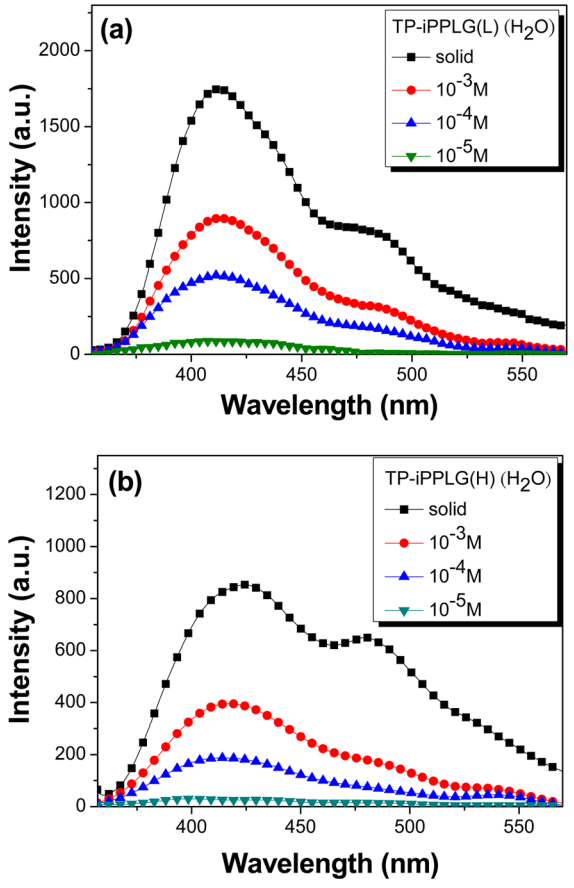

Figure 8. (a) Concentration effect on the PL emission spectra of (a) TP-iPPLG(L) and (b) TP-iPPLG(H) solutions and solids (λ_{ex} = 325 nm).

dx.doi.org/10.1021/ma500886v | Macromolecules 2014, 47, 4037−4047

All emission spectra in Figure 8 consist of two overlapping bands, with the short-wavelength monomer emission at 420 nm and the long-wavelength aggregate emission shown as the right shoulder of the monomer emission. The aggregate emission became significant for the solid polymers, which is conceivable in considering the feasible intermolecular aggregations of the TP terminals in the condensed solid states. Comparatively, the solid TP-iPPLG(L) emits with higher intensity than the high-MW TP-iPPLG(H), which can be further certified from the respective Φ_F values of 0.29 and 0.23 measured from integrating sphere. With higher content of fluorescent TP unit, TP-iPPLG(L) therefore emits more efficiently than TP-iPPLG(H) with lower TP content. The relative intensity between the aggregate and the monomer emissions is also an index for the intermolecular aggregation of the TP units in TP-iPPLG(L) and TP-iPPLG(H). The solid emission spectrum of TP-iPPLG(H) (Figure 8b) reveals a higher aggregate/monomer emission ratio than the spectrum of TP-iPPLG(L) (Figure 8a). As concluded above, intermolecular aggregation of TP terminals is more effectively blocked when they are linked to the large α-helical rod; therefore, with less fraction of α-helical chain TP-iPPLG(L) therefore emits with lower aggregate/monomer ratio than TP-iPPLG(H) with higher fraction of α-helix.

Aggregates formed in solvent/nonsolvent can be used to identify the AEE effect; here, DMF was used as nonsolvent to induce aggregation of TP-iPPLGs in water. Upon excitation at 325 nm, dilute aqueous solutions (10^{-4} M) of TP-iPPLGs already emitted with discernible intensity (Figure 9), and increasing DMF in the solution (while keeping concentration of TP-iPPLGs at 10^{-4} M) caused little but progressive gain on the emission intensity. Upon increasing concentration of TP-iPPLGs, the monomer emission peak progressively shifted to higher wavelengths. Suggestively, the fluorescent TP unit may adopt a more planar geometry with increasing steric constraint imposed by aggregates formed in the solutions. The emission spectra in Figure 9 indicated that both TP-iPPLG(L) and TP-iPPLG(H) are AEE-active materials.

The α-helix of poly(L-glutamic acid) species were reported to undergo a helix-to-coil transition at pH value of 6.18.[39,40] A similar transition was observed in β-CD-grafted PPLG,[16] however, at a higher pH range in between 11 and 11.5 due to the steric hindrance or the stable helical structure inherited by the β-CD grafts. For TP-iPPLGs, similar conformational transformation induced in the highly alkaline solution was expected to vary the AIE-related emission behavior due to different aggregation states accompanied by conformational change. Indeed, the aqueous TP-iPPLG(L) showed a progressive transformation on the emission peaks upon increasing pHs from 7 to 13.3 (Figure 10). Emission spectra of the aqueous TP-iPPLG(L) at pH 2 and 7 are essentially the same; however, when NaOH was gradually added to the aqueous TP-iPPLG(L) solution, the initial monomer emission was continuously transformed into a major aggregate emission. Among all, the major transformation occurred at a pH value somewhere between pH 11 and pH 13.3. At pH 13.3, the TP-iPPLG(L) solution emitted with a large aggregate emission, whose intensity is almost 3-fold to the intensity obtained at pH 7. In highly alkaline solution, the main chain of TP-iPPLG(L) underwent a helix-to-coil transformation, and once again, the easy intermolecular aggregation of TP terminals in the random coil chains was responsible for the highly fluorescent

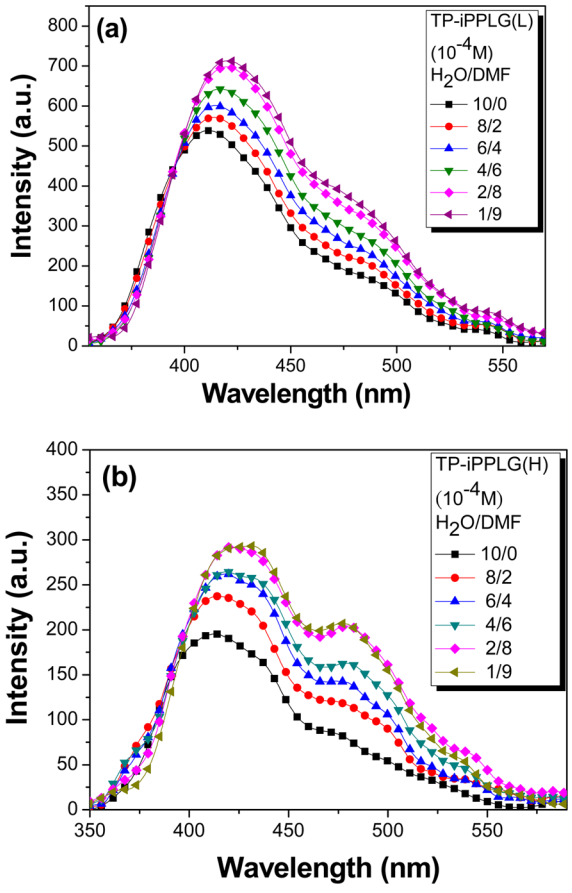

Figure 9. Emission spectra of (a) TP-iPPLG(L) and (b) TP-iPPLG(H) in water/DMF mixtures of different compositions (λ_{ex} = 325 nm).

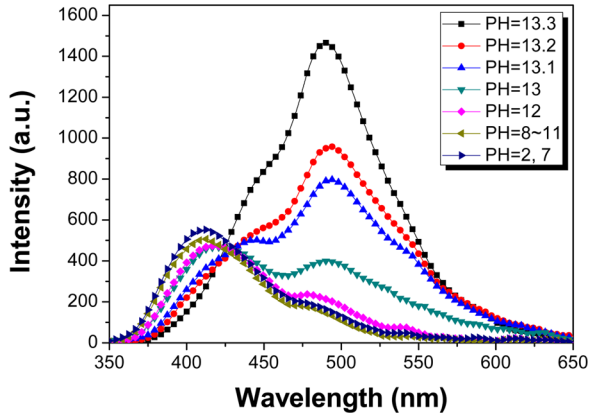

Figure 10. PL emission spectra of the aqueous TP-iPPLG(L) solutions with different pH values (λ_{ex} = 325 nm).

aggregation emission observed in the spectra. The corresponding conformational transformation was characterized next.

Conformational Transformation of the TP-iPPLG(L) Polymer in Water. We recorded circular dichroism spectra to characterize the conformational transformation of the water-soluble TP-iPPLG(L) polymer in alkaline aqueous solution. The α-helical structure was characterized by a triply inflected spectrum, corresponding to two negative bands at 208 and 222 nm and a strong positive band at 192 nm. The β-sheet structure was characterized by a negative minimum band near 218 nm and a positive maximum near 198 nm. The random coil

dx.doi.org/10.1021/ma500886v | Macromolecules 2014, 47, 4037−4047

structure was characterized by a small positive band at 218 nm and a negative band near 200 nm.[39] The fourth principal structure of the C_{10}-helix (i.e., a repetitive H-bonded ring containing 10 atoms)[41] possesses a tighter, more elongated, and higher potential energy than the α-helix structure (C_{13}-helix). Nevertheless, the C_{10}-helix was characterized by a small positive band at 195 nm, with a smaller intensity and a much lower ellipticity ratio ($[\theta]_{222}/[\theta]_{208}$) than that of the α-helix.[42]

Next, we tested the effect of pH on the conformation of TP-iPPLG(L). The circular dichroism spectra in Figure 11 display

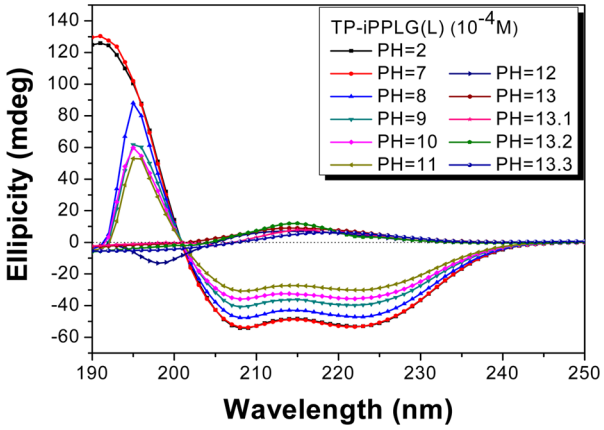

Figure 11. Effect of pH on the circular dichroism spectrum of TP-iPPLG(L) in NaOH solution.

the pH-induced conformational changes of the TP-iPPLG(L) solutions. By increasing the basicity of the solution from pH 7 to 11, we observed a slight variation on the ratio $[\theta]_{222}/[\theta]_{208}$, indicating that there are only minor conformational change involved in this pH range. The polymer chains should remain as a helical mixture of α-helix and C_{10}-helix structures.[39] Nevertheless, the major conformational transformation occurred in highly alkaline solutions with pH > 12; at this stage, the triply inflected spectrum reduced to a doubly inflected dichroic spectrum. The α-helix of the TP-iPPLG(L) polymer was converted to a random coil conformation by the alkaline NaOH. The intramolecular H-bonds involved in the α-helical chains were dissociated in the highly alkaline environment.

The conformational change in the alkaline solution is therefore correlated with the AEE-related emission behavior, which is closely associated with the extent of molecular approaches (aggregation) of the TP fluorophores in TP-iPPLG. The geometrical factor affecting the extent of intermolecular aggregation was conceptually depicted in Scheme 1. In the solution state, the TP fluorophores with a molecular width of 9 Å can be more effectively isolated from other TP units if they are connected to a large α-helical chain with a diameter of 25 Å (the diameters of the α-helix are in the ranges of 15−26 Å[43−45]) than those in the flexible random coil or in the β-sheet chains. In acidic and neutral solutions (from pH 2 to pH 7), the TP-iPPLG chains mainly existed in the large α-helical conformation. The TP terminal in the large α-helical chains are more isolate from other TP terminals, resulting in the monomer emission with low emission intensity. In contrast, the TP-iPPLG(L) chains transformed into the flexible random coil structure in the alkaline solution. The TP terminals in the random coil conformation underwent easy intermolecular association, resulting in the major aggregate emission with the intensity much higher than those in the acidic and neutral solutions. Effect of chain conformation on the AEE-related emission behavior is thus verified.

With the ionic pendant group, the present TP-iPPLG system exhibits the helix-to-random coil transformation in alkaline solution. However, the previous system of TP-2PBLG[32] was reported to proceed this conformational transformation at acidic environment (pH = 2 in THF−H_2O (v/v = 1/9)). For the neutral TP-2PBLG, acidic species added in the solution tend to penetrate into the peptide chain, dissociating the intramolecular H bonds dominant in the α-helical structure of TP-2PBLG, to result in random-coil chains. But for the present TP-iPPLG, the ionic sulfonate pendant groups greatly enhance the stability of the α-helical chains in the acid media. The ionic sulfonate groups are considered to serve as efficient electrostatic shields, protecting the interior peptide chains from the attacks of the acidic species. In strong acidic media, the sulfonate pendant groups may just be protonated to result in sulfonic acid groups with sustained stability in the acid media.

The quantum efficiencies (Φ_Fs) of the aqueous solutions (10^{-4} M) (Table 3) at different pH values are in the ranges

Table 3. Quantum Efficiency (Φ_F) Measured from the Solution[a] at Different pHs

TP-iPPLG(L)	solution (10^{-4} M)					
pH	7−11	12	13	13.1	13.2	13.3
Φ_F (%)	7	6.8	8.7	12.7	14.2	18.7

[a]Quantum yield, obtained by using quinine sulfate as refer ence standard (10^{-4} M in 1 N H_2SO_4).

from 0.07 to 0.187. As common dye for biomaterials, fluorescein and rodamine 101 have extremely high Φ_Fs of 0.95 (in aqueous 0.1 M NaOH solution, pH = 13) and 1.0 (in ethanol),[46] respectively. The weak solution emission efficiency of TP-iPPLG(L) is typical of AIE-active materials since free molecular rotation in the mobile solution state activates the nonradiative decay pathways, resulting in the weak solution emission.

TP-iPPLG(L) as Sensor for Bovine Serum Albumin. Among varieties of serum albumin, bovine serum albumin (BSA)[47] is the most studied one in the biochemistry or biomedical science due to its structural similarity with human serum albumin (HSA).[48] As a large globular protein (66 kDa) consisting of 583 amino acid residues in a single polypeptide chain, BSA was often used as a binding material with certain dyes and probes, which provides fluorescence for the study of binding mechanisms.[49]

With the inferior quantum efficiency, TP-iPPLG(L) can still be used as probe for detecting BSA. In this case, when BSA was added to the alkaline (pH = 13.3) solution of TP-iPPLG(L), emission of the solution mixtures became weaker (Figure 12) with increasing BSA content from 0 to 5 mg/mL. Comparatively, the long-wavelength aggregate emission exhibits more drastic intensity reduction compared to the monomer emission at short-wavelength region. Suggestively, intermolecular aggregation of the TP terminals is largely hampered, rendering in the reduced aggregate emission, when the TP-iPPLG(L) chains bind to the large protein chains of BSA. The random coil chain, as the main structure of TP-iPPLG(L) in the alkaline solution, preferably binds to BSA, resulting in stable homogeneous solution for measurement. In contrast, no such measurement is possible for the acidic and neutral TP-iPPLG solutions because in this case adding BSA caused immediate

dx.doi.org/10.1021/ma500886v | Macromolecules 2014, 47, 4037−4047

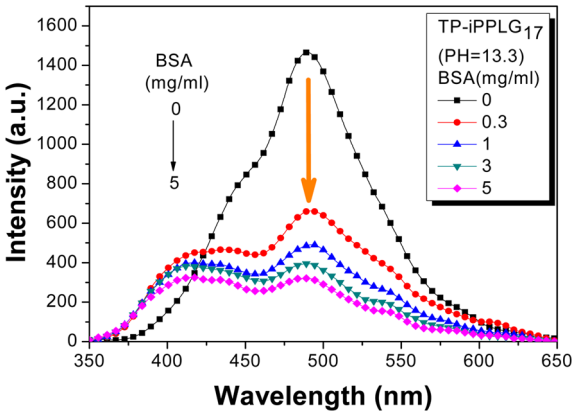

Figure 12. Emission spectra of the alkaline TP-iPPLG(L) solution (10^{-4} M, pH = 13.3) at different amounts of BSA from 0 to 5 mg/mL (λ_{ex} = 325 nm).

precipitation of the reaction products. Water-insoluble products were thus produced when BSA reacted to TP-iPPLG(L) chains in the rigid α-helix or β-sheet structures.

CONCLUSIONS

A new series of water-soluble TP-iPPLG polymers containing an AEE-active fluorescent terminal and ionic side groups can be successfully prepared from a two-step reaction scheme, including the ring-opening polymerization of PLG-NCA monomer, initiated by an AIE-active initiator of TP-NH_2, to generate the neutral TP-PPLG and the following click reaction on TP-PPLG to introduce the desired ionic pendant groups. The TP-iPPLG polymers are AEE-active materials according to the emission behavior in H_2O/DMF solution mixtures.

Ionic pendant group and MW of the polypeptides are found to affect the secondary structure of the resulting peptide chain. The ionic sulfonate pendant group in TP-iPPLGs enhances the content of the α-helical structure when compared to the neutral precursors of TP-PPLGs. With higher MW, solid TP-iPPLG(H) also possesses higher fraction of α-helical chains as compared to low-MW TP-iPPLG(L). Since α-helical chains are efficient in blocking the intermolecular aggregation of the TP units, the emission spectrum of solid TP-iPPLG(H) therefore contains less aggregate to monomer emission ratio as compared to TP-iPPLG(L) with lower α-helix content.

The ionic sulfonate pendant groups of TP-iPPLG protect the peptide main chain from attacking of the acidic species. Therefore, TP-iPPLGs are rather stable in acidic media; however, the stable α-helical structures are transformed into random coil chains in the highly alkaline solution. Emission of the alkaline TP-iPPLG solution contains a large aggregate emission with the intensity much higher than the emission in the acidic and neutral media. Effect of secondary structure on the AEE-activity was therefore demonstrated. The alkaline solution of TP-iPPLG(L) can be a probe for the detection of BSA, and the corresponding emission spectra exhibit the large reduction of the aggregate emission with increasing dosage of BSA in the solution.

ASSOCIATED CONTENT

Supporting Information

Figures S1–S7. This material is available free of charge via the Internet at http://pubs.acs.org.

AUTHOR INFORMATION

Corresponding Author

*E-mail jlhong@mail.nsysu.edu.tw; Tel +886-7-5252000 ext 4065 (J.-L.H.).

Notes

The authors declare no competing financial interest.

ACKNOWLEDGMENTS

This study was supported financially by the National Science Council, Taiwan, Republic of China, under Contracts NSC 102-2221-E-110-084-MY3 and NSC 102-2221-E-110-080-.

REFERENCES

(1) Kricheldorf, H. R. *Angew. Chem., Int. Ed.* **2006**, *45*, 5752–5784.
(2) Deming, T. J. *Prog. Polym. Sci.* **2007**, *32*, 858–875.
(3) Deming, T. J. In *Peptide Hybrid Polymers; Polypeptide and Polypeptide Hybrid Copolymer Synthesis via NCA Polymerization*; Klok, H. A., Schlaad, H., Eds.; Springer: Berlin, 2006; pp 1–18.
(4) Munoz, V.; Serrano, L. *Nat. Struct. Biol.* **1994**, *1*, 399–409.
(5) Fiori, W. R.; Lundberg, K. M.; Millhauser, G. L. *Nat. Struct. Biol.* **1994**, *1*, 374–377.
(6) Goodman, C. M.; Choi, S.; Shandler, S.; DeGrado, W. F. *Nat. Chem. Biol.* **2007**, *3*, 252–262.
(7) Fezoui1, Y.; Hartley, D. M.; Walsh1, D. M.; Selkoe1, D. J.; Osterhout, J. J.; Teplow, D. B. *Nat. Struct. Biol.* **2000**, *7*, 1095–1099.
(8) Drin, G.; Casellal, J.-F.; Gautier, R.; Boehmer, T.; Schwartz, T. U.; Drin, B. A. *Nat. Struct. Mol. Biol.* **2007**, *14*, 138–146.
(9) Bryson, J. W.; Betz, S. F.; Lu, H. S.; Suich, D. J.; Zhou, H. X.; O'Neil, K. T.; DeGrado, W. F. *Science* **1995**, *270*, 935–941.
(10) Bang, D.; Gribenko, A. V.; Tereshko, V.; Kossiakoff, A. A.; Kent, S. B.; Makhatadze, G. I. *Nat. Chem. Biol.* **2006**, *2*, 139–143.
(11) Zhang, S. G. *Nat. Biotechnol.* **2003**, *21*, 1171–1178.
(12) Hartgerink, J. D.; Beniash, E.; Stupp, S. I. *Science* **2001**, *294*, 1684–1688.
(13) Nowak1, A. P.; Breedveld, V.; Pakstis, L.; Ozbas, B.; Pine, D. J.; Pochan, D.; Deming, T. J. *Nature* **2002**, *417*, 424–428.
(14) Lu, H.; Wang, J.; Bai, Y.; Lang, J. W.; Liu, S.; Lin, Y.; Cheng, J. *Nat. Commun.* **2011**, *2*, 1–9.
(15) Zhang, Y.; Lu, H.; Lin, Y.; Cheng, J. *Macromolecules* **2011**, *44*, 6641–6644.
(16) Lin, Y. C.; Wang, P. I.; Kuo, S. W. *Soft Matter* **2012**, *8*, 9676–9684.
(17) Doty, P.; Bradbury, J. H.; Holtzer, A. M. *J. Am. Chem. Soc.* **1956**, *78*, 947–954.
(18) Pokorná, V.; Výprachtický, D.; Pecka, J. *Macromol. Biosci.* **2001**, *1*, 185–190.
(19) Kim, K. T.; Park, C.; Vandermeulen, G. W. M.; Rider, D. A.; Kim, C.; Winnik, M. A.; Manners, I. *Angew. Chem., Int. Ed.* **2005**, *117*, 8178–8182.
(20) Rubatat, L.; Kong, X.; Jenekhe, S. A.; Ruokolainen, J.; Hojeij, M.; Mezzenga, R. *Macromolecules* **2008**, *41*, 1846–1852.
(21) Luo, J.; Xie, Z.; Lam, J. W. Y.; Cheng, L.; Chen, H.; Qiu, C.; Kwok, H. S.; Zhan, X.; Liu, Y.; Zhu, D.; Tang, B. Z. *Chem. Commun.* **2001**, 1740–1741.
(22) Tang, B. Z.; Zhan, X.; Yu, G.; Lee, P. P. S.; Liu, Y.; Zhu, D. *J. Mater. Chem.* **2001**, *11*, 2974–2981.
(23) *Aggregation-Induced Emission: Fundamentals*; Qin, A., Tang, B. Z., Eds.; John Wiley & Sons, Ltd.: New York, 2013.
(24) Liu, J.; Lam, J. W. Y.; Tang, B. Z. *J. Inorg. Organomet. Polym.* **2009**, *19*, 249–285.
(25) Hong, y.; Lam, J. W. Y.; Tang, B. Z. *Chem. Commun.* **2009**, 4332–4353.
(26) Wu, J.; Liu, W.; Ge, J.; Zhang, H.; Wang, P. *Chem. Soc. Rev.* **2011**, *40*, 3483–3495.
(27) Hong, Y.; Lam, J. W. Y.; Tang, B. Z. *Chem. Soc. Rev.* **2011**, *40*, 5361–5388.

(28) Qin, A.; Lam, J. W. Y.; Tang, B. Z. *Prog. Polym. Sci.* **2012**, *37*, 182−209.
(29) Chien, R. H.; Lai, C. T.; Hong, J. L. *J. Phys. Chem. C* **2011**, *115*, 5958−5965.
(30) Lai, C. T.; Hong, J. L. *J. Phys. Chem. B* **2010**, *114*, 10302−10310.
(31) Lai, C. T.; Chien, R. H.; Kuo, S. W.; Hong, J. L. *Macromolecules* **2011**, *44*, 6546−6556.
(32) Li, S. T.; Lin, Y. C.; Kuo, S. W.; Chuang, W. T.; Hong, J. L. *Polym. Chem.* **2012**, *3*, 2393−2402.
(33) Lin, Y. C.; Kuo, S. W. *Polym. Chem.* **2012**, *3*, 162−171.
(34) Lin, Y. C.; Kuo, S. W. *Polym. Chem.* **2012**, *3*, 882−891.
(35) Papadopoulos, P.; Floudas, G.; Klok, H. A.; Schnell, I.; Pakula, T. *Biomacromolecules* **2004**, *5*, 81−91.
(36) Murata, K.; Katoh, E.; Kuroki, S.; Ando, I. *J. Mol. Struct.* **2004**, *689*, 223.
(37) Kricheldorf, H. R.; Muller, D. *Macromolecules* **1983**, *16*, 615.
(38) Sela, M.; Katchalski, E. *Adv. Protein Chem.* **1959**, *14*, 391−478.
(39) Hwang, J.; Deming, T. J. *Biomacromolecules* **2001**, *2*, 17−21.
(40) Zimmermann, R.; Kratzmu, T.; Erickson, D.; Li, D.; Braun, H. G.; Werner, C. *Langmuir* **2004**, *20*, 2369−2374.
(41) Ananda, K.; Vasudev, P. G.; Sengupta, A.; Poopathi, K. M.; Shamala, R. N.; Balaram, P. *J. Am. Chem. Soc.* **2005**, *127*, 16668−16674.
(42) Toniolo, C.; Polese, A.; Formaggio, F.; Crisma, M.; Kamphuis, J. *J. Am. Chem. Soc.* **1996**, *118*, 2744−2745.
(43) Torii, T.; Yamashita, T.; Horie, K. *Eur. Polym. J.* **1993**, *29*, 1265−1270.
(44) Doty, P.; Bradbury, J. H.; Holtzer, A. M. *J. Am. Chem. Soc.* **1956**, *78*, 947−954.
(45) Bovey, F. A.; Tiers, G. V. D. *Adv. Polym. Sci.* **1963**, *3*, 139−195.
(46) Lakowicz, J. R. *Principles of Fluorescence Spectroscopy*, 2nd ed; Kluwer Academic/Plenum Publishers: New York, 1999; p 53.
(47) Moriyama, Y.; Ohta, D.; Hadiya, K.; Mitsui, Y.; Takeda, K. *J. Protein Chem.* **1996**, *15*, 265−272.
(48) He, X. M.; Carter, D. C. *Nature* **1992**, *358*, 209−215.
(49) Zhang, Y. Z.; Zhou, B.; Zhang, X. P.; Huang, P.; Li, C. H.; Liu, Y. *J. Hazard. Mater.* **2009**, *163*, 1345−1352.